



# Modeling and simulation to optimize direct power control of DFIG in variable-speed pumped-storage power plant using teaching–learning-based optimization technique

Seyed Mohammad Hassan Hosseini<sup>1</sup> · Alireza Rezvani<sup>2</sup>

Published online: 5 May 2020

© Springer-Verlag GmbH Germany, part of Springer Nature 2020

## Abstract

The issues related to the optimal control of large-scale storage systems in electric power systems such as pumped storage (PS) plant have turned into vital challenges in the way of integrating renewable energy sources into power systems to provide reliable and economical electric energy. In this regard, this paper uses the direct power control strategy to model and simulate a variable-speed PS plant, which includes a doubly fed induction generator (DFIG). The active and the reactive power of the stator would be able to be controlled, separately. This approach has a better dynamic performance compared to other methods, while it would be quite simple to implement. But there are some shortfalls with this method, such as high ripple relating to the active power as well as reactive power together with the current harmonics. In this respect, the space vector modulation (SVM) is applied to eliminate these shortfalls. In the proposed control technique, including SVM, the dynamic performance of the studied DFIG unit is controlled using the proportional–integral (PI) controller. It should be noted that the teaching–learning-based optimization (TLBO) method is employed to tune the PI controller for controlling the DFIG system in the PS plant. Finally, in order to validate the performance of the suggested framework, a comparison is made between the results obtained by the TLBO and the ones reported by other optimization methods. The obtained results using the TLBO algorithm indicate better performance of the PI controller to reduce the ripples of the active and reactive power of the stator as well as the harmonic power.

**Keywords** Pumped-storage power plant · Doubly fed induction generator · Teaching–learning-based optimization · Imperialist competitive algorithm · Particle swarm optimization algorithm

## 1 Introduction

Electrical energy must be essentially generated and consumed, simultaneously. Since the large-scale storage of energy would be economical, an effective and efficient solution would be using PS generation technology. In the past, almost every pump-turbine was composed of synchronous motors and generators operating with the network frequency, and thus, the speed was constant. Nowadays, PS

plants with doubly fed induction machine (variable speed) have been enhanced with advanced power electronic devices, not only can help control the system frequency, but also will result in the power system stability. The efficiency and the performance of such systems would be substantially promoted by employing machines of variable-speed type (Dadfar et al. 2019).

The dynamic behavior of  $2 \times 320$  MW PS plant of the variable-speed type has been modeled and analyzed in Pannatier et al. (2010), while the plant comprises a hydraulic system as well as other assets, such as electrical supplies, control units besides the rotating inertias. In this respect, the hydraulic system and the electrical parts of the PS plant have been modeled, while the complete models have been employed to characterize the dynamic performance of the control method in either generating or pumping states when the set points relating to the active power vary.

---

Communicated by V. Loia.

✉ Seyed Mohammad Hassan Hosseini  
smhh110@azad.ac.ir

<sup>1</sup> Department of Electrical Engineering, South Tehran Branch, Islamic Azad University, Tehran, Iran

<sup>2</sup> Department of Electrical Engineering, Saveh Branch, Islamic Azad University, Saveh, Iran

Recently, in variable-speed units, AC/DC/AC back-to-back converters are used instead of cycloconverters. The reason could be described as no need for any starter for starting up the power plant and better capability to control the power plant. An AC/DC/AC back-to-back converter is composed of a rectifier set of AC/DC type, which is linked to the network through a transformer and a dihedral inverter of DC/AC type directly joined to the rotor windings of the studied DFIM (Dendouga et al. 2007).

The control method used in this paper is direct power control (DPC) approach where the active as well as the reactive power of the stator can be controlled directly and separately. The dynamic behavior of the mentioned approach is more desirable compared to other methods, while its implementation is very simple, but it has several defects such as high active and reactive power ripple and current harmonics. So, the space vector modulation (SVM) is used to eliminate these defects. To implement the SVM method, a proportional–integral (PI) controller has been used. The precise adjustment of the coefficients in the PI controller is very important because the systems which are controlled have high orders and time delays (Ou and Lin 2006).

Today, proportional–integral derivative (PID) controllers have turned into the most employed ones compared to other types. There are several merits with this type of controllers, such as robust performance for different states of operation and a straightforward design (Chatterjee and Mukherjee 2016). PID controllers for grid-side converter (GSC) and rotor-side converter (RSC) control the transacting active and reactive powers between the DFIG and the main grid. The purpose of the PID controllers is to maximize the extracted power from the PS plant (Yamamoto and Motoyoshi 1991; Pena et al. 1996; Muller et al. 2002; Tapia et al. 2003; Tang and Xu 1995). Appropriately determining the parameters of the controller is vital to make better system stability and operation. So far, various heuristic optimization methods have been used to enhance the response of the DFIG system through tuning the PID controller gains.

It is noted that most of the research works in the literature have analyzed the tuning of controller coefficients of DFIG-based wind turbines and only a few number of papers have focused on the application of DFIGs in PS plants. Therefore, for applying this method to the PS plants, a brief review is carried out on the previously published research works on tuning the DFIG controller's coefficients. The operation of the system majorly depends upon the GSC controller actions. Thus, the optimization of parameters has been done for GSC PI controllers to achieve an optimal performance of the DFIG.

Genetic algorithm (GA)-based optimization approach is presented in Rezvani et al. (2016) to get the gains of

controllers for the RSC with the primary target of enhancing the DFIG capability. It is applied to determine the controller parameters of static var compensator in Ju et al. (1996), and for tuning the parameters of hydro generator in Lansberry and Wozniak (1994). Hasanien and Muyeen (2012) used the GA to optimally design the control system of a frequency converter, and the PSO algorithm has been employed in Qiao et al. (2006) to specify the optimal values of the parameters of DFIG-based WT's controller and in Abido (2002) for the automatic voltage controller application. The PSO algorithm has also been used in Wu et al. (2007) to tune the gains of the DFIG controller aimed at reducing the rotor's current and enhancing the small-signal stability.

Intelligent optimization methods such as PSO, imperialist competitive algorithm (ICA) and teaching–learning-based optimization (TLBO) have been already used to adjust the parameters of PI controller for optimizing the active power as well as the reactive power control relating to the machine, and results of these three methods have been compared. This paper impalements optimization method-based PSO, ICA and TLBO as components of searching algorithm. In this regard, Chatterjee and Mukherjee (2016) utilized the TLBO method, which is on the basis of the classroom environment idea to transfer knowledge from one person to others. In this optimization technique, the global solution is obtained utilizing a population of solutions like other approaches based on population. It is also noted that the population includes the learners. In this respect, various topics recommended to the learners indicate the design variables in this optimization algorithm, while the learners' result denotes the value of the fitness function. In this paper, the main aim is to design a novel method for tuning the controller's coefficients of a PS plant equipped with a DFIG. The proposed technique is appropriate to be used in PS plant applications. The effect of the aforementioned methods is investigated in order to improve the stability of the Siah Bisheh PS plant located in the Northern Iran. In this regard, the studied power system is modeled by using MATLAB Software, while it is connected to the infinite bus through a 150-km double-circuit line. Simulation results show that the TLBO algorithm-based PI controller effectively works in reducing the ripples of the active and reactive power of the stator and harmonic current. The obtained results also verify that the TLBO method algorithm is better than the PSO and ICA methods for the dynamic performance of the PS power plant.

To this end, the DFIG model together with its relations is presented. Afterward, the steps of implementing the DPC technique are mentioned. Then, the model of the hydraulic part of the PS power plant is presented that is composed of a turbine, a penstock and a surge tank. At the next section,

PSO, ICA and TLBO algorithms are presented, and at the end, the proposed model and the simulation results for these three methods will be compared.

## 2 Mathematical model of DFIG

The DFIG structure is composed of different parts as a wound-rotor induction machine coupled with an AC–DC–AC convertor. It is noted that the winding of the stator is just connected to the main grid, and the variable frequency is fed to the rotor using convertors. This advantage is due to the optimized PS plant speed and the reduced mechanical stress on the PS plant over the extreme weather like storms. As it is quite obvious, the highest power generated by the DFIG is directly dependent upon the PS plant. In between, the convertor of power electronic type is able to either produce or consume the reactive power. Thus, no extra reactive compensator is needed. Besides, the controller existing at the rotor side of the machine enables the control of electromagnetic torque. This can be carried out by controlling the injected rotor voltage. To this end, the reference speed supplied by the DFIG system must be tracked by the electromagnetic torque. Through this control strategy, the highest power can be extracted during the DFIG's variable-speed operation. It should be noticed that the grid-connected stator using the convertor at the grid side is utilized to control the voltage of the DC link and transact the reactive power with the main grid. The mathematical representation of the DFIG using the d–q reference frame can be indicated as follows (Abad et al. 2007):

Voltage equations:

$$\begin{aligned} u_{ds} &= r_s i_{ds} + p\psi_{ds} - \omega_s \psi_{qs} \\ u_{qs} &= r_s i_{qs} + p\psi_{qs} + \omega_s \psi_{ds} \\ u_{dr} &= r_r i_{dr} + p\psi_{dr} - (\omega_s - \omega_r) \psi_{qr} \\ u_{qr} &= r_r i_{qr} + p\psi_{qr} + (\omega_s - \omega_r) \psi_{dr} \end{aligned} \quad (1)$$

Linkage flux equations:

$$\begin{aligned} \psi_{ds} &= L_s i_{ds} + L_m i_{dr} \\ \psi_{qs} &= L_s i_{qs} + L_m i_{qr} \\ \psi_{dr} &= L_r i_{dr} + L_m i_{ds} \\ \psi_{qr} &= L_r i_{qr} + L_m i_{qs} \end{aligned} \quad (2)$$

In the above equations,  $u_{ds}$ ,  $u_{qs}$  and  $i_{ds}$ ,  $i_{qs}$  denote the d and q components of the stator's voltage and current, respectively.  $u_{dr}$ ,  $u_{qr}$  and  $i_{dr}$ ,  $i_{qr}$  are the d and q components relating to the rotor's voltage and current, respectively.  $\psi_{ds}$ ,  $\psi_{qs}$ ,  $\psi_{dr}$  and  $\psi_{qr}$  also indicate the d and q components of stator and rotor flux linkage, respectively.  $L_s = L_1 + L_m$  and  $L_r = L_2 + L_m$ , while  $L_1$  and  $L_2$  are rotor and stator leakage inductances, respectively, and  $L_m$

denotes the mutual inductance. Besides, the stator and rotor resistances are represented by  $r_s$  and  $r_r$ , respectively.

## 3 Direct power control method

The general equations of the active and reactive power relating to the stator are stated as follows (Ou and Lin 2006):

$$P_s = \frac{3}{2} (u_{ds} i_{ds} - u_{qs} i_{qs}) \quad (3)$$

$$Q_s = \frac{3}{2} (u_{qs} i_{ds} - u_{ds} i_{qs}) \quad (4)$$

The equations relating to the active and reactive power of the stator are revised and rewritten in terms of rotor and stator fluxes and can be represented as below (Ou and Lin 2006; Yamamoto and Motoyoshi 1991):

$$P_s = \frac{3}{2} \frac{L_m}{\sigma L_s L_r} \omega_s |\psi_s| |\psi_r| \sin \delta \quad (5)$$

$$Q_s = \frac{3}{2} \frac{\omega_s}{\sigma L_s} |\psi_s| \left[ \frac{L_h}{L_r} |\psi_s| - |\psi_r| \cos \delta \right] \quad (6)$$

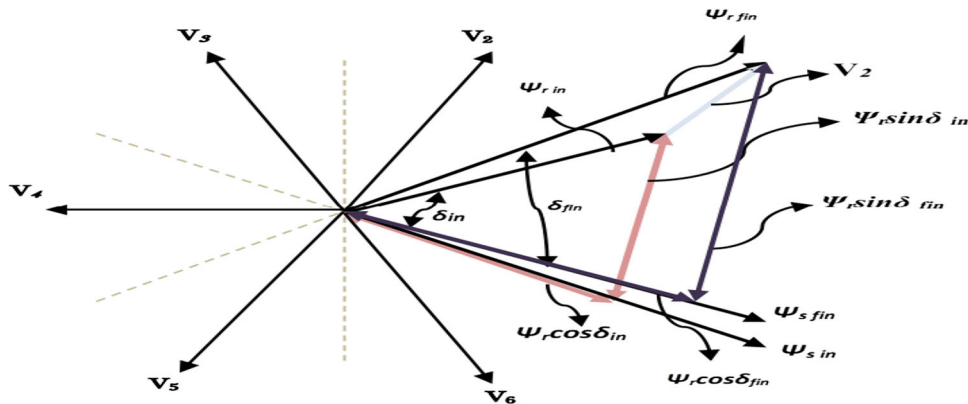
Having taken into consideration the above-represented formulations, the active and reactive powers of the stator vary by the variations in the relative angle between the flux vectors and the flux amplitudes of the stator and rotor. As the flux amplitude of the stator is constant, the active and reactive powers of the stator are dependent upon the angle between the flux vectors of the stator and rotor as well as the flux amplitude of the rotor. Moreover, it should be noted that due to the constant speed of the stator rotating flux vector, using each of the eight vectors of voltage relating to the dihedron convertor leads to a new angle  $\delta$  (Chatterjee and Mukherjee 2016).

Figure 1 shows the effect of voltage vector  $V_2$  in the generating mode (that rotor flux is ahead of the stator flux) at sub-synchronous speeds.

As Fig. 1 depicts, vector  $|\psi_r| \cos \delta$  as well as vector  $|\psi_r| \sin \delta$  has been raised resulting in raising the active power and lowering the reactive power as shown in (5) and (6), respectively. It is worth mentioning that the same investigation can be made for different sectors to observe the impacts of other vectors produced by the inverter on the active and reactive power of the stator. Table 1 represents the switching table of the DPC technique in generating mode and sub-synchronous speed.

The block diagram relating to the DPC of a DFIG is indicated in Fig. 2. As can be observed in Fig. 2, a comparison is made between the reference values pertaining to the active and reactive power and the estimated ones and they are ultimately assigned to be used in the hysteresis

**Fig. 1** The representation of the impact of the vector of inverter output on the active and reactive power of the stator



**Table 1** Switching table of DPC method in generating mode

EP	1	0	- 1	1	0	- 1
EQ	1			- 1		
<i>Sector number</i>						
1	V <sub>3</sub>	V <sub>7</sub>	V <sub>5</sub>	V <sub>2</sub>	V <sub>0</sub>	V <sub>6</sub>
2	V <sub>4</sub>	V <sub>0</sub>	V <sub>6</sub>	V <sub>3</sub>	V <sub>7</sub>	V <sub>1</sub>
3	V <sub>5</sub>	V <sub>7</sub>	V <sub>1</sub>	V <sub>4</sub>	V <sub>0</sub>	V <sub>2</sub>
4	V <sub>6</sub>	V <sub>0</sub>	V <sub>2</sub>	V <sub>5</sub>	V <sub>7</sub>	V <sub>3</sub>
5	V <sub>1</sub>	V <sub>7</sub>	V <sub>3</sub>	V <sub>6</sub>	V <sub>0</sub>	V <sub>4</sub>
6	V <sub>2</sub>	V <sub>0</sub>	V <sub>4</sub>	V <sub>1</sub>	V <sub>7</sub>	V <sub>5</sub>

the convertor located at the grid side. PI controllers are employed to carry out the SVM technique. In this respect, the block diagram relating to the control system of the GSC is depicted in Fig. 3. As this figure shows, there are three PI controllers: voltage controller, power controller and current controller. For the sake of enhancing the performance of the proposed control system, the PI controller’s coefficients need to be accurately adjusted. Three intelligent optimization methods, namely PSO, ICA and TLBO, are used for tuning the coefficients. In the next section, the results of using three methods are presented and compared.

controller. The output of the hysteresis controller together with the sector number, where the rotor flux exists, is assigned as the inputs in the switching table. The table is used to specify the proper voltage vector, and after that, pulses  $s_a$ ,  $s_b$  and  $s_c$  are given to the dihedral voltage source converter (VSC) (Yamamoto and Motoyoshi 1991).

Controlling the machine is done using the DPC method, and the SVM is utilized in the presented control system of

### 4 Hydraulic model of system

This section presents the mathematical model relating to the hydraulic parts of the PS plant, such as penstock, the surge tank and the turbine. Finally, the general model as a combination of these models is presented. Figure 4 shows the connection of these components.

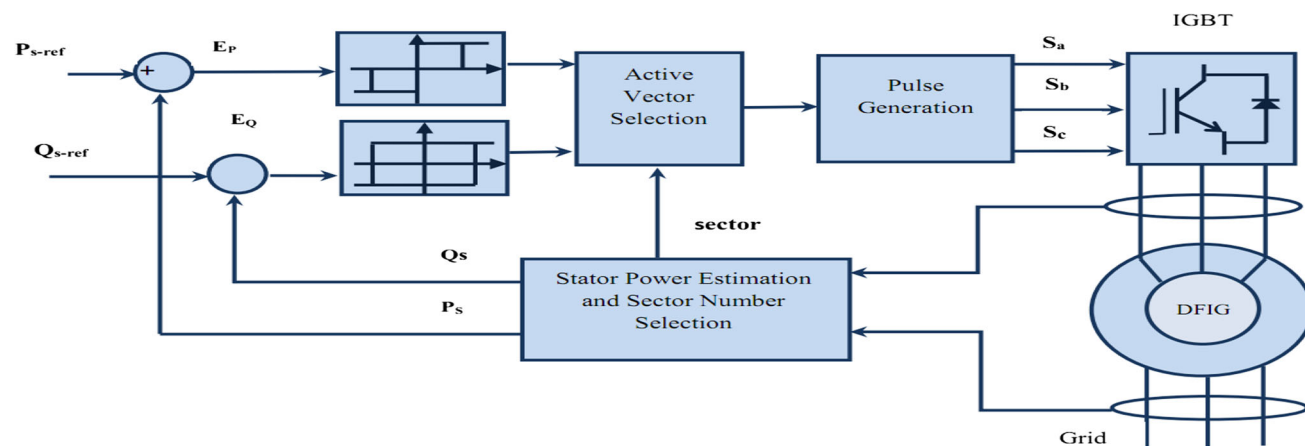


**Fig. 2** Block diagram of direct power control in the doubly fed induction machine

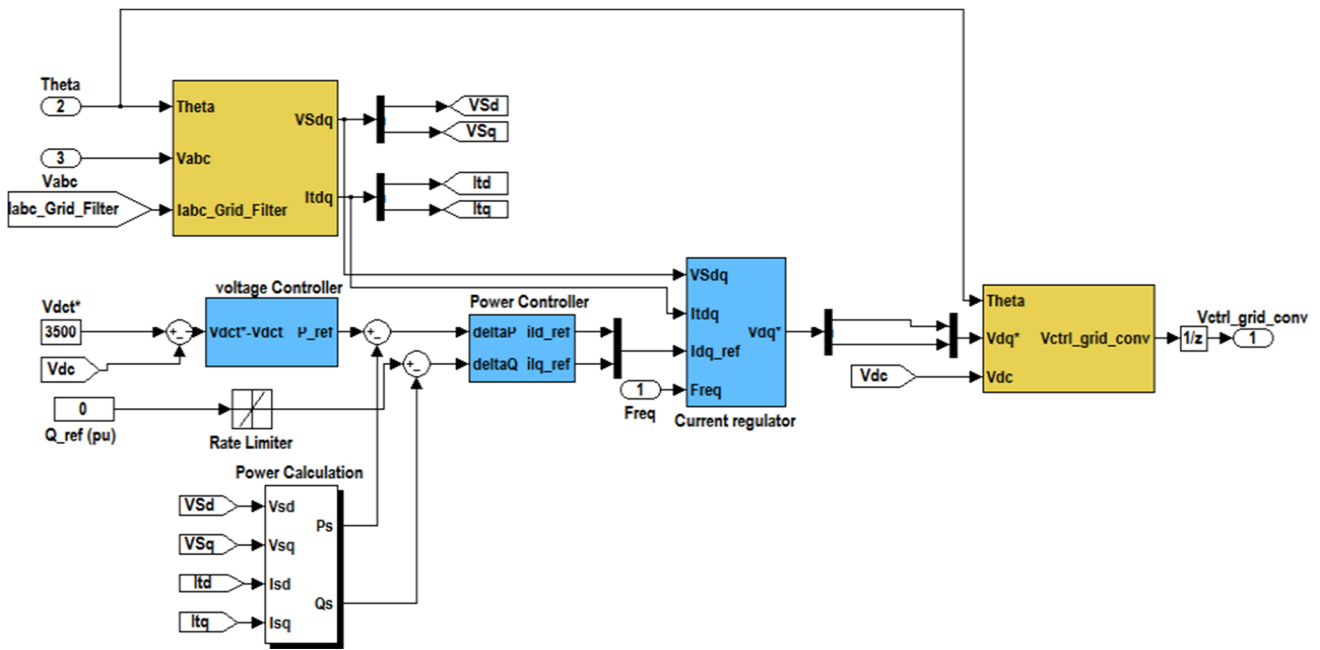
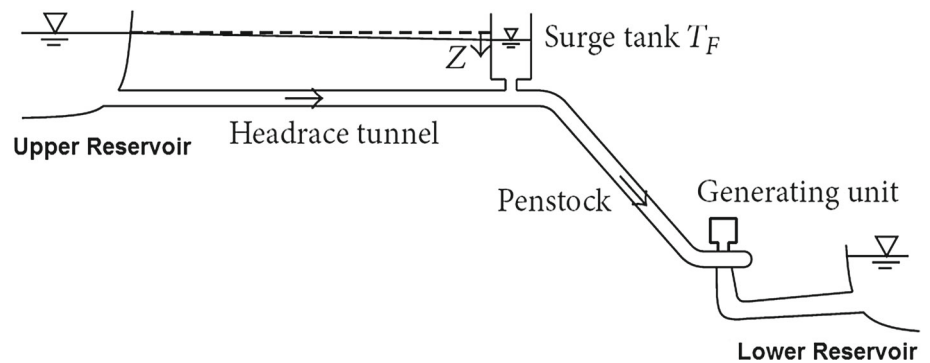


Fig. 3 Block diagram of the GSC control system

Fig. 4 A simple view of hydraulic components of a PS plant



### 4.1 Dynamic model of penstock

The influencing items in the basic equations can be stated as the water speed in the penstock, water acceleration and the power generation of the turbine, taking into account the flowing water volume and the penstock’s nonelasticity as below (Schmidt et al. 2017; Hosseini and Semsar 2016).

$$(H_0 - H - H_f)\rho gh = \rho AL \frac{dU}{dt}$$

$$H_f = f \times \frac{L}{D} \times \frac{U^2}{2g} = f_p \times Q^2 \tag{7}$$

$$f_p = \frac{L}{D} \times \frac{f}{2g} \times \frac{1}{A^2}$$

where  $H_0$ ,  $H$  and  $H_f$  are, respectively, the static head of water column, the static head at the turbine admission and the conduit head losses due to the friction. Also,  $U$ ,  $L$  and  $D$  are, respectively, the water velocity inside the penstock, the

length of the conduit and the conduit diameter.  $f$  and  $f_p$  are also the friction factor and the conduit head loss coefficient. The water starting time ( $T_w$ ) is the time required for the water in height  $H_{base}$  to reach speed  $U_{base}$  in the penstock. The water starting time is expressed as follows (Schmidt et al. 2017; Hosseini and Semsar 2016):

$$T_w = \frac{LQ_{base}}{H_{base}gA} = \frac{LU_{base}}{H_{base}g} \tag{8}$$

### 4.2 Surge tank model

The elastic feature of waterways wall creates ambulatory waves in the water; this phenomenon is known as water hammer or ram impact. Water hammer occurs when the water pressure changes (higher or lower than the normal pressure) that are in fact due to the sudden change in the water flow rate.

The two main reasons that can cause this phenomenon in the power plants’ water way are:

- Opening and closing the power plant inlet valve
- Change in the guide vane opening

The surge tank is used in hydro power plants to omit the damaging impacts caused by the water hammer. Regardless of the head losses in the tunnel of a rigid system, the impacts of oscillation period and the storage constant in the surge tank are calculated using the following relations (Schmidt et al. 2017; Hosseini and Semsar 2016):

$$T_{st} = 2\pi\sqrt{\frac{LA_s}{gA}} \tag{9}$$

$$C_s = \frac{A_s H_{base}}{Q_{base}}$$

In these relations,  $L$ ,  $A_s$  and  $A$  are, respectively, the length of conduit between the reservoir to surge tank, surge tank area and conduit area.

### 4.3 Turbine model

Turbine mechanical power in the steady state is calculated by the following relation (Schmidt et al. 2017; Hosseini and Semsar 2016):

$$P_m = \eta Q \rho g H \tag{10}$$

where  $P_m, \eta, Q$  and  $\rho$  are, respectively, the turbine power output, the turbine efficiency, the turbine flow rate and the water density.

Two changes must be applied in the above equation in real conditions:

- Turbine damping affected by the guide vane opening and rotor speed variations should be considered.
- In real terms, turbine no-load flow ( $Q_{nL}$ ) should be subtracted from the main flow so that the effective flow in power creation would be obtained that is due to losses.

Thus, the turbine power output equation can be rewritten as follows:

$$P_m = A_t H(Q - Q_{nL}) - D_n G \Delta \omega \tag{11}$$

In this relation,  $D_n$  is the turbine damping factor and  $A_t$  is the turbine gain factor that is obtained by the following equation:

$$A_t = \frac{1}{G_{f1} - G_{nL}} \times \frac{\text{Turbine power}}{\text{Generator power}} \tag{12}$$

The turbine flow rate equation is expressed as follows:

$$Q = G\sqrt{H} \tag{13}$$

The block diagram of IEEE nonlinear model for a turbine with a penstock considering the nonelastic water column is depicted in Fig. 5 (Hosseini and Semsar 2016).

## 5 PSO algorithm

The PSO method is an optimization algorithm which is on the basis of the social behavior of birds’ movement. This algorithm was presented first by Kennedy and Eberhart (1995) and Rezvani et al. (2019). In the PSO algorithm, several particles are created as the initial solutions in the search space. The movement of these particles in the search space is completely stochastic and influenced by its experience and other particles’ experience. In other words, the motion vector of each particle is determined randomly by the outcome of the movement toward the best location that the particle has been there ( $L_{best}$ ) and the movement toward the best location between the whole particles ( $G_{best}$ ) (Kennedy and Eberhart 1995). Suppose  $x_i$  is the location of particle  $i$  and  $v_i$  is the velocity of this particle. In this case, the motion vector of every particle will be calculated according to the following relations (Kennedy and Eberhart 1995; Rezvani et al. 2019).

$$v_i(t + 1) = W \times v_i(t) + C_1 \times R_1 \times (x_i^{L_{best}}(t) - x_i(t)) + C_2 \times R_2 \times (x^{G_{best}}(t) - x_i(t)) \tag{14}$$

$$x_i(t + 1) = v_i(t + 1) + x_i(t) \tag{15}$$

In (14),  $C_1, C_2$  and  $W$  are the coefficient of motion toward  $L_{best}$ , the coefficient of motion toward  $G_{best}$  and the inertia coefficient, respectively, and they are the algorithm parameters.  $R_1$  and  $R_2$  denote random numbers that increase the algorithm search capability. This algorithm is expressed as a flowchart in Fig. 6 (Farajdadian and Hosseini 2019; Cai et al. 2010).

## 6 Imperialist competitive algorithm (ICA)

This algorithm is an evolutionary algorithm and starts with the determination of a random population, where each member is called a country. In this regard, some elements of the population as the best ones are chosen as imperialists and the remaining countries are considered colonies. The entire power of each empire is calculated as the sum of the imperialist country’s power plus a percentage of its colonies’ average power. The empire’s survival will depend upon its ability to attract rival empires colonies. Gradually, in this competition, larger empires power will be added and weak empires will be removed. Empires have to improve

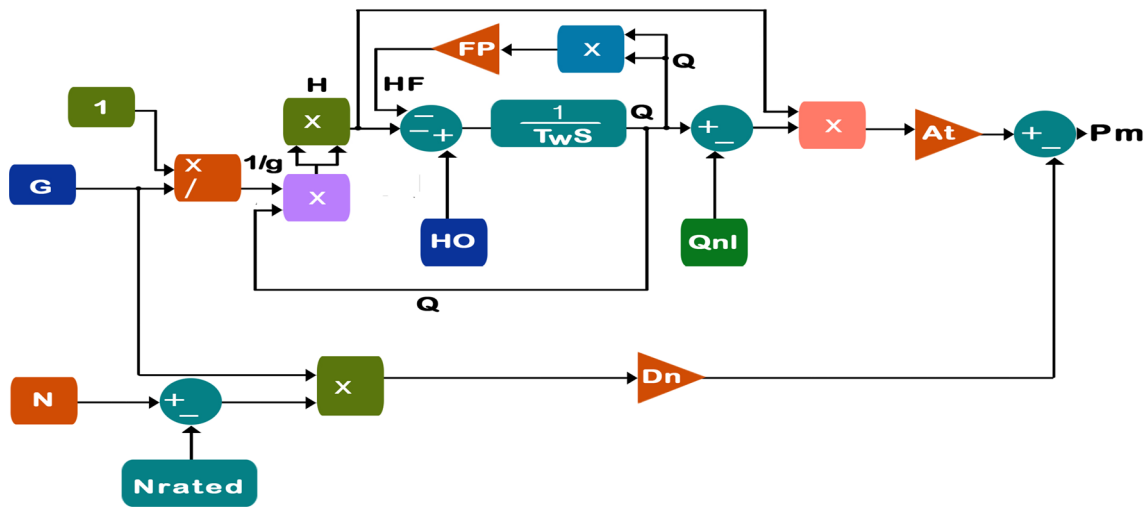


Fig. 5 Block diagram of nonlinear model of the turbine and penstock

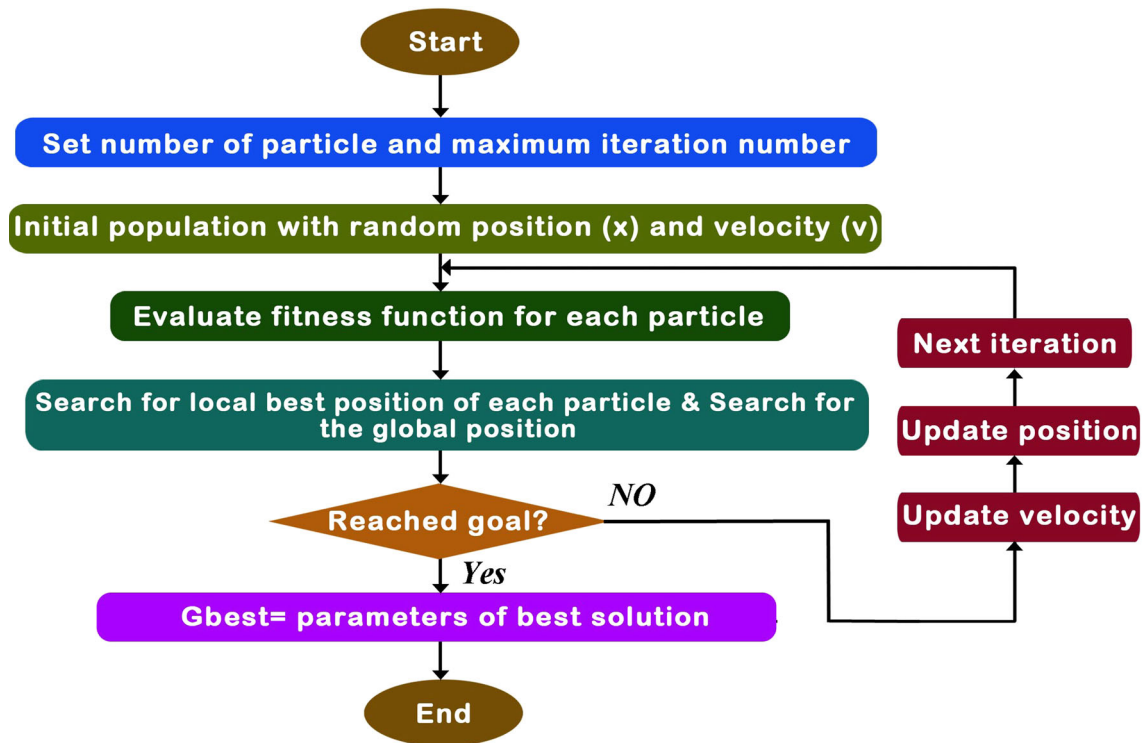


Fig. 6 Flowchart of PSO algorithm

their colonies to increase their power, and this leads to the nearness of imperialist's power to their colonies power. The last stage of the competition relates to the time with merely one empire, in which the imperialist and colonies situation are very close (Atashpaz and Lucas 2007). This algorithm is shown as a flowchart in Fig. 7.

### 7 Teaching-learning-based optimization (TLBO)

The principles of the TLBO method are based upon the procedures related to the teaching and learning in the classroom as stated in Rao et al. (2011) and Rai (2017). In this regard, the descriptions of the TLBO method are given in the following. The reason beyond choosing the teaching-learning procedures in the classroom is that it is the

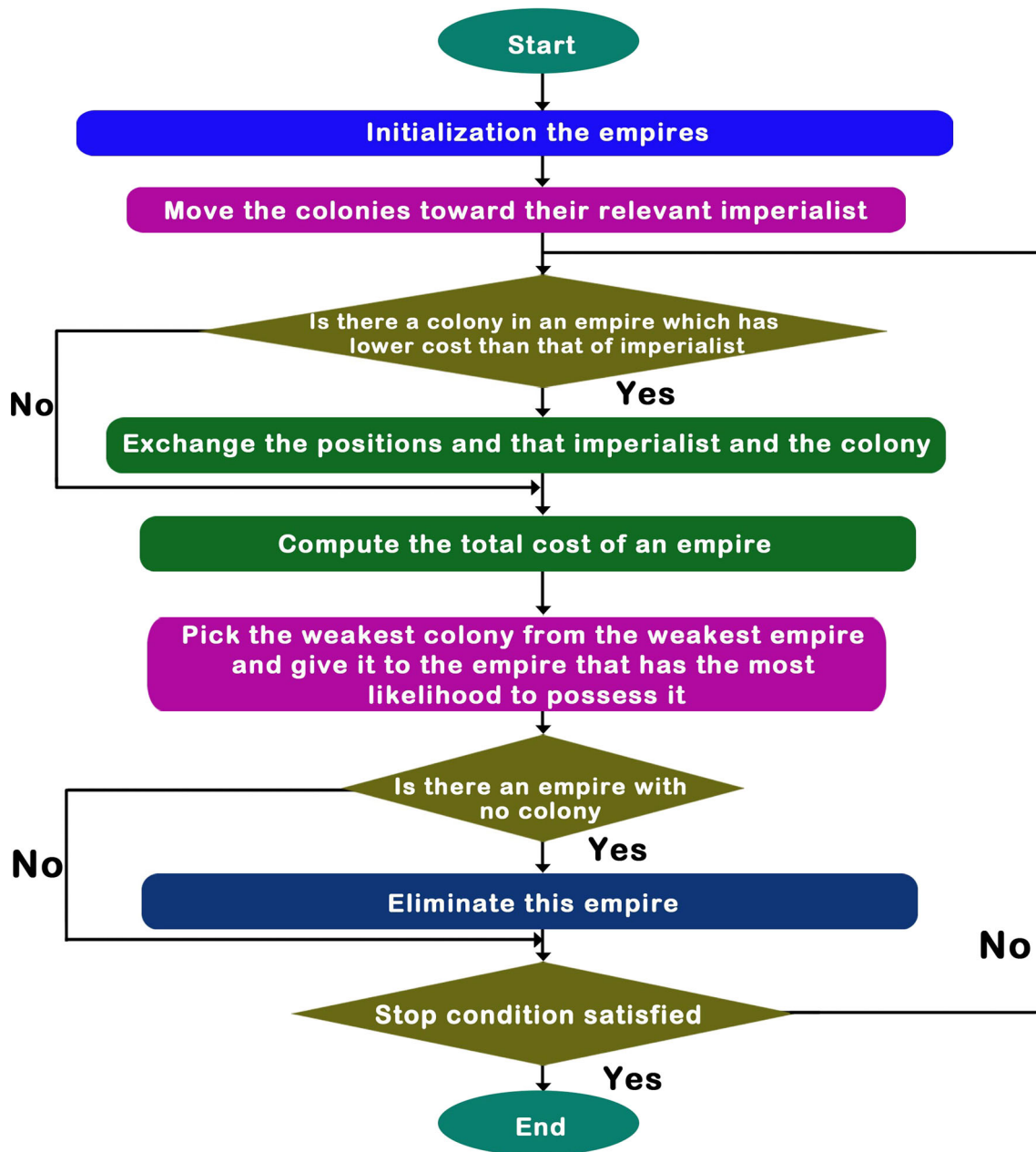


Fig. 7 Flowchart of ICA algorithm

most efficient tool in the education system to make the expected reforms in students. Equivalently, the TLBO method is enhanced by the impact of a teacher on the student's (learner's) output. In this optimization algorithm, the output is the mark or grade got by the learner. It should be noted that the teacher has taken into consideration a deeply educated individual teaching students in a way they can enhance their results. Therefore, learning of students (learners) would be improved in case they get desirable outputs. Additionally, learners learn through interacting with others which possibly leads to more desirable results.

TLBO is regarded as an optimization algorithm which is on the basis of population, while the set of learners are taken into account as the population and the courses offered to the learners are taken into account as design variables. Besides, it should be noted that the result obtained by the students indicates the fitness function of the studied optimization problem. However, there are two main sections in the TLBO method: the "teacher phase" and the "learner phase."



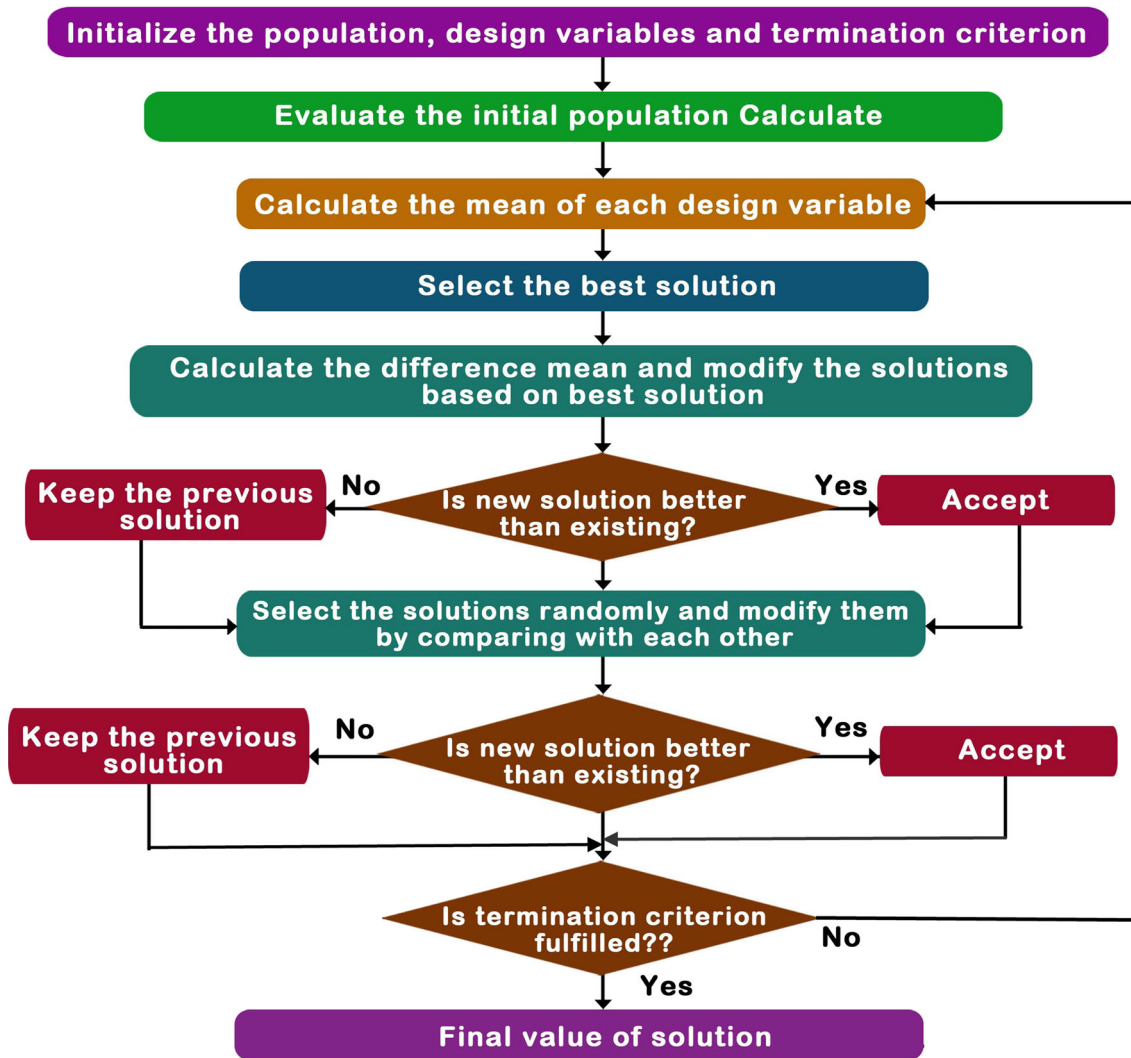


Fig. 8 Flowchart of TLBO algorithm

### 7.1 Teacher phase

This part includes the education of the students by the teacher in order to raise the mean learning value of the class based on the quality of the education. Assume the number of design variables  $m$  offered to  $n$  students,  $T$  as the output of the teacher and  $M$  as the mean result at each instant  $i$ ; then, the value of  $T$  is intended to fit the value of  $M$  to its own level. In this respect, the new mean is introduced as  $M_{new}$ . Equation (16) states the difference between  $M$  and  $M_{new}$ :

$$\text{difference\_mean}_i = r_i(M_{new} - T_F M_i) \tag{16}$$

where  $r_i$  denotes a random variable produced in  $[0\ 1]$  range and the teaching factor is indicated by  $T_F$ , determining the mean value to be altered that its value would be 1 or 2. Equation (17) declares the definition of  $T_F$ :

$$T_F = \text{round}[1 + \text{rand}(0, 1) \times (2 - 1)] \tag{17}$$

Equation (18) states the adjustment of the current solution belonging to the difference:

$$X_{new,i} = X_{old,i} + \text{difference\_mean} \tag{18}$$

The values of  $r_i$  and  $T_F$  are produced randomly within the optimization method and impact the performance of the TLBO method, while they are not taken into account as the input to the TLBO method, just in contrary to cognitive and social parameters and inertia weight in the PSO algorithm or colony size and limit in the ABC and mutation probabilities as well as crossover in the GA. Thus, adjusting  $r_i$  and  $T_F$  is not needed, while it is necessary to adjust the usual control parameters, such as the number of generations as well as the population size. In all optimization algorithms, which are on the basis of population, the usual control parameters are considered a requirement. Hence,

**Table 2** Hydraulic characteristics of Siah Bisheh power plant

Section	Genus	Length (m)	Diameter (m)	Flow (m <sup>3</sup> /s)	Speed (m/s)	Friction factor
Left waterway	Metallic	902	5	130	6.62	0.008
	Concrete	1969	5.6	130	5.09	0.012
Right waterway	Metallic	882	5	130	6.62	0.008
	Concrete	1926	5.6	130	5.09	0.012

**Table 3** Turbine characteristics of Siah Bisheh power plant

Rated flow (m <sup>3</sup> /s)	Rated power (MW)	Nominal height (m)	No-load flow (m <sup>3</sup> /s)	Speed (rpm)
59.49	260.35	476.17	8	500

**Table 4** Characteristics of converter and transformer of Siah Bisheh power plant

Rated power (MVA)	Input voltage (KV)	Output voltage (KV)	Transformer connection (m <sup>3</sup> /s)	Frequency (Hz)
26.7	18	3	Yy0	50

the TLBO method can be taken into consideration as an algorithm-specific parameter-less one.

### 7.2 Learner phase

This section includes the reciprocal communication of the students (learners) that may lead to rise in the knowledge of the students. The random interaction of the learners promotes imparting the knowledge since a student (learner) can learn a new thing provided that other students know more, and Fig. 8 shows different stages of the TLBO method.

## 8 Objective function

Figure 3 depicts the block diagram of the GSC control system. As can be observed from this figure, there are three PI controllers: voltage controller, the power controller and the current controller. The performance of the converter highly relies upon the control system, such that in case the controllers have not been adjusted appropriately, it would be probable to enhance the GSC performance over transient disturbances. The objective of the PSO, ICA and TLBO methods has been assigned to the model as determining the optimal parameters of the three PI controllers, or in other words, three proportional gains ( $K_P$ ) and three integral gains ( $K_I$ ) in order to specify the optimal value of the fitness functions. The objective functions presented below are employed to assess the quality of the gains adjustment in order to enhance the performance of the system over transient disturbances. It can be considered that the objective functions are stated using the weighted

sum of the normalized mean square error (NMSE) deviations between the output variables of the plant and the desired values.

$$j = \text{NMSE} = \int_0^t \frac{\sum (P_{\text{OUT}} - P_{\text{ref}})^2}{\sum (P_{\text{ref}})^2} dt \tag{19}$$

Constraints of proposed objective function are stated as follows:

$$K_{P\text{min}} \leq K_P \leq K_{P\text{max}} \tag{20}$$

$$K_{I\text{min}} \leq K_I \leq K_{I\text{max}} \tag{21}$$

## 9 Case study

The location of the Siah Bisheh PS plant is in the north of Iran between Karaj and Chalous near the Siah Bisheh village. The purpose beyond making this power plant is balancing Iran’s power network consumption. The characteristics of the power plant are given in Tables 2, 3,

**Table 5** Electrical specifications of DFIG relating to Siah Bisheh power plant

Nominal power (MVA)	300.6
Nominal effective voltage (KV)	18
Nominal frequency (Hz)	50
Stator resistance ( $\Omega$ )	0.015
Stator self-inductance (mH)	0.342
Rotor resistance ( $\Omega$ )	0.0431
Rotor self-inductance (mH)	0.342
Mutual inductance (H)	0.0171
Pole pairs	3

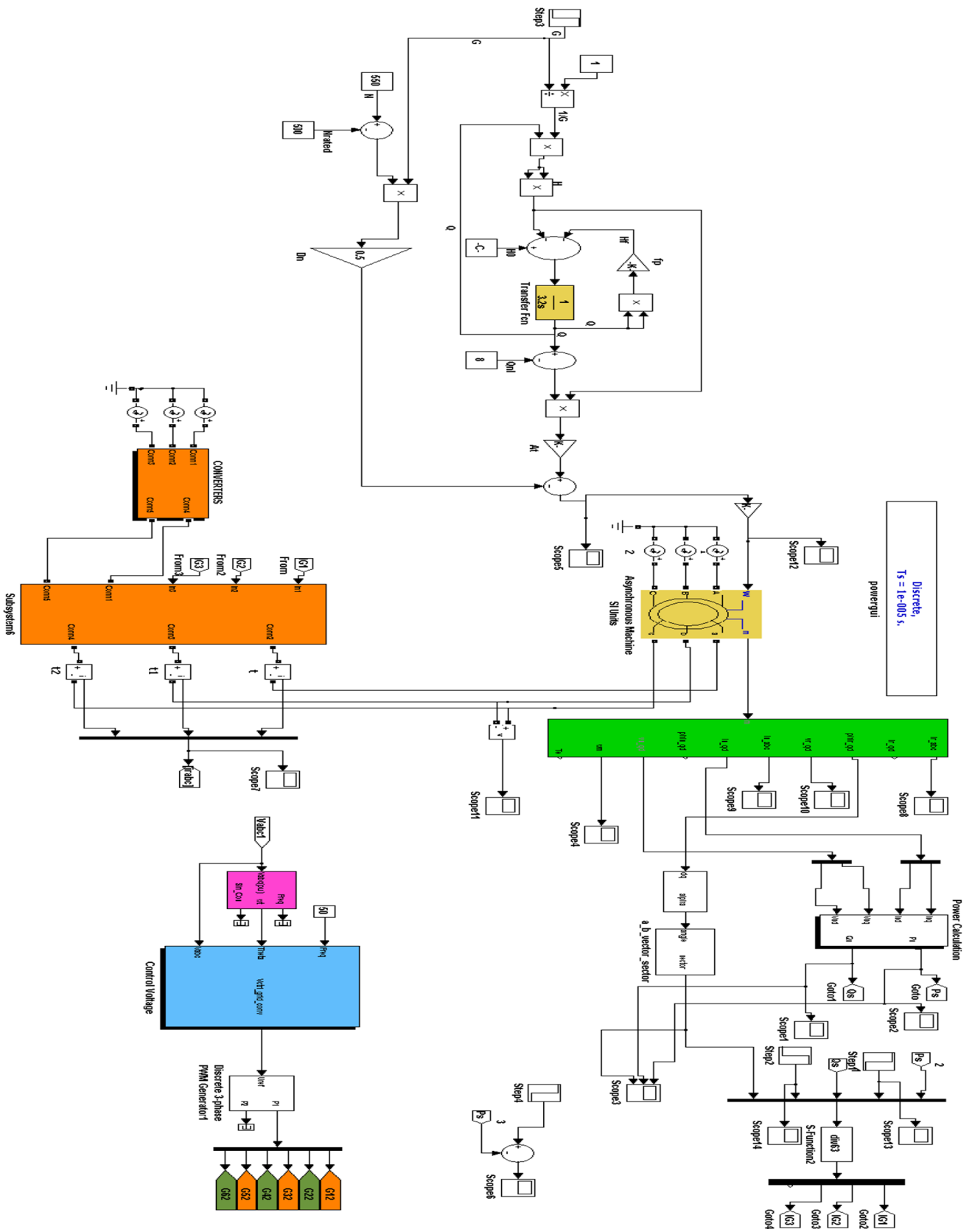


Fig. 9 The proposed system

**Table 6** PSO setting specifications

Number of iterations	Initial population	Inertia factor	Self-learning factor	Collective learning factor
8	8	0.7298	1.495	1.495

**Table 7** ICA setting specifications

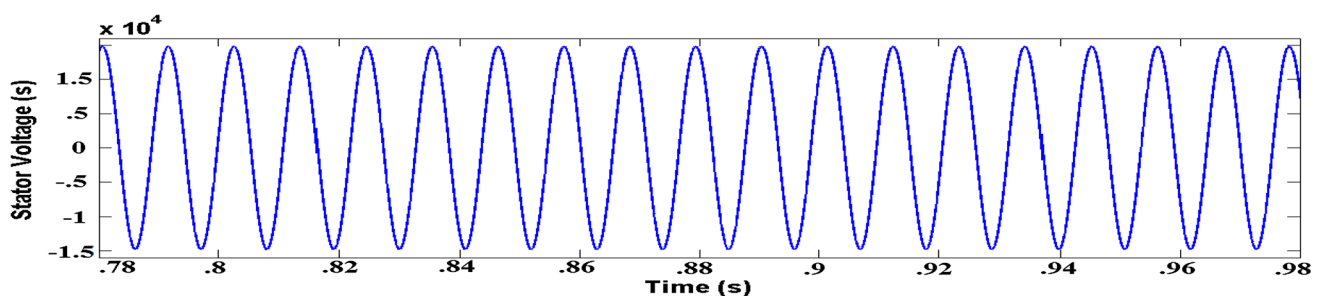
Number of iterations	Number of countries	Number of imperialists	Number of colonies	Revolution factor	Colony power factor
8	9	3	6	0.1	0.1

**Table 8** TLBO setting specifications

Number of students	Number of iterations	Teaching step	Teaching factor
4	8	1	1

**Table 9** Comparison between PI controller coefficients in different methods

Method	Method based on PI	Method based on PSO	Method based on ICA	Method based on TLBO
<b>Controller coefficients</b>				
<b>Voltage controller</b>				
$K_P$	0.02	0.021	0.017	0.013
$K_I$	0.6	0.725	0.81	0.92
<b>Power controller</b>				
$K_P$	5	6.14	6.1	5.87
$K_I$	500	536.21	530	525
<b>Current controller</b>				
$K_P$	5	6.03	5.7	5.4
$K_I$	500	517.2	530.6	537.8

**Fig. 10** Stator voltage of DFIG

4 and 5. This power plant consists of four synchronous units of 250 MW (Hosseini and Eslami 2019). In this paper, we have studied one of them when the asynchronous machine is substituted with the DFIG.

## 9.1 Proposed model presentation

The general model which is simulated includes a DFIG in a PS power plant. Also, the hydraulic part of the power plant is simulated by using IEEE nonlinear model for the

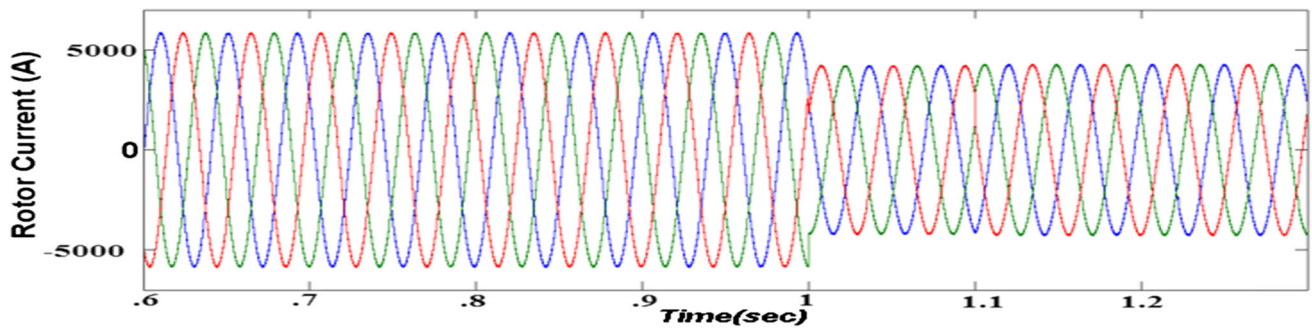


Fig. 11 Rotor current of DFIG

penstock and turbine as depicted in Fig. 9. The stator and the electrical network are directly connected, while a back-to-back dihybrid converter is used to connect the rotor to the power grid. It is noteworthy that the converter comprises a GSC as well as a machine-side converter joined together through a DC link capacitor. Indeed, the DC voltage produced by the rectifier set is fed to the inverter set.

## 10 Simulation results

The doubly-fed induction machine together with the hydraulic part of the PS power plant is simulated using MATLAB software. The DFIG characteristics have been represented in Table 5. The setting specifications of methods, i.e. PSO, ICA and TLBO are presented in Tables 6, 7 and 8. As mentioned above, there are three PI controllers: the voltage controller, the power controller and the current controller. To enhance the performance of the proposed control system, the PI controller's coefficients need to be accurately adjusted. Three intelligent optimization methods are used for tuning the coefficients. In this section, the results obtained from these methods are presented and compared. Also, the coefficients of the PI controller obtained using the three intelligent methods are presented in Table 9. Figures 10 and 11 show the stator voltage and rotor current in DFIG when the ICA method is used to adjust the PI controller's coefficients.

Figures 12, 13, 14 and 15 illustrate the variations in the stator active power, efficiency of the stator active power, the variations in stator reactive power and the efficiency of stator reactive power when PSO, ICA and TLBO algorithms are used to adjust the proportional–integral coefficients. It is noted that the reference active power is a step input with an initial value of 130 MW reduced to 120 MW at  $T = 1$  (s). Hence, the active power control of the DFIG has reached 108 MW from 118 MW using the mentioned optimization algorithms by the DPC technique that well tracks the reference value. The reference reactive power of

the stator is a step input with an initial value of 50 MVAR increased to 66 MVAR at  $T = 1.5$  (s). It is noted that the reactive power control of the DFIG using the DPC technique has been well carried out, while it well tracks the reference reactive power.

The active and reactive power output relating to the stator in the method on the basis of the aforementioned algorithms can be seen in Figs. 12a, 13a, 14a and 15a. It can be observed in these figures that the ripple of the active and reactive power output relating to the stator reduces more using the TLBO method in comparison with the PSO and ICA. It means the power quality improvement. Indeed, this object represents the higher efficiency of the TLBO method in precisely tuning the PI controller coefficients compared to the PSO and ICA.

It can be derived that the efficiency of the stator's active power varies between 92% and 94%, whereas the TLBO algorithm's efficiency is 96% as shown Figs. 12b, 13b, 14b and 15b. It can be derived that the efficiency of the stator's reactive power varies between 86 and 93%, whereas the TLBO algorithm's efficiency is 94% as shown in Figs. 12d, 13d, 14d and 15d.

Furthermore, Figs. 16 and 17 show the total harmonic distortion (THD) value for rotor and stator current in three methods. Figure 18 depicts the voltage of the DC link applied to the inverter. Lower THD in the PS plant means a higher power factor, lower peak currents and a higher efficiency. It is noted in Figs. 16 and 17 that the TLBO algorithm has a better performance than PSO and ICA in terms of the THD.

It can be deduced that the presented control frameworks on the basis of the TLBO lead to a rational dynamic performance. The behavior of the system in the case of using the TLBO, PSO and ICA for self-tuning the controllers is indicated in Table 10. This table represents the THD measurements in the three-phase grid voltage and grid current waveforms, as well as the three-phase rotor voltage and current wave forms, ripple percentage of the stator's active and reactive power and also the THD in the three algorithms. However, it is noticed that the TLBO method

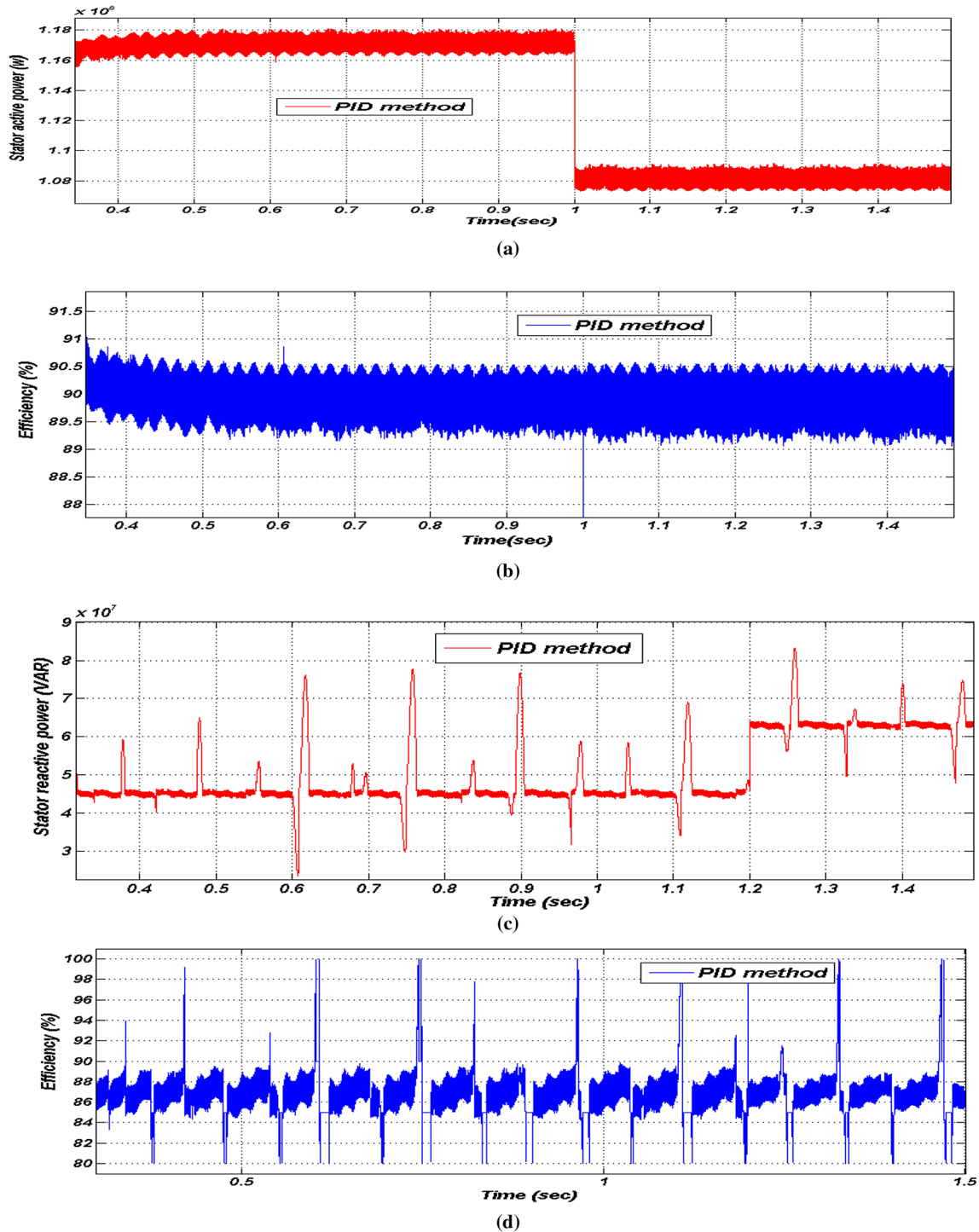


**Fig. 12** **a** Variations in stator active power in the method based on PID controller; **b** efficiency of the stator's active power in the method based on PID controller; **c** variations in the stator's reactive power in the method based on PID controller; **d** efficiency of the stator's reactive power in the method based on PID controller

shows an effective performance in determining the optimal parameters relating to the PID controller and enhances the transient behavior of the wave energy system during different operating conditions.

The important point to be noted in the simulation results is that because of long run time in the three methods, a small number of iterations and initial population have been considered. The simulation run time in the method based

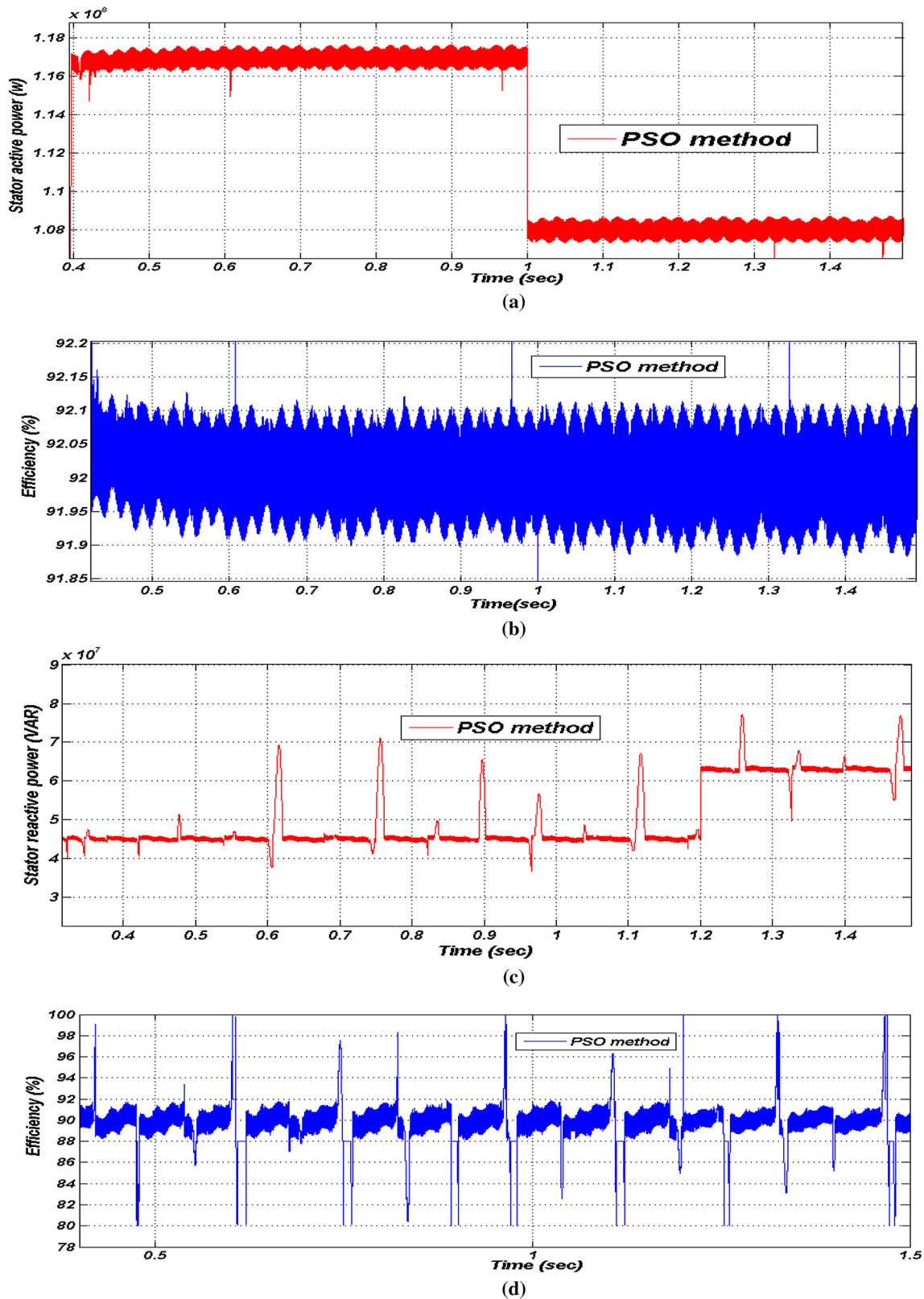


**Fig. 13** **a** Variations in the stator’s active power in the method based on PSO; **b** efficiency of the stator’s active power in the method based on PSO; **c** variations in the stator’s reactive power in the method based on PSO; **d** efficiency of the stator’s reactive power in the method based on PSO

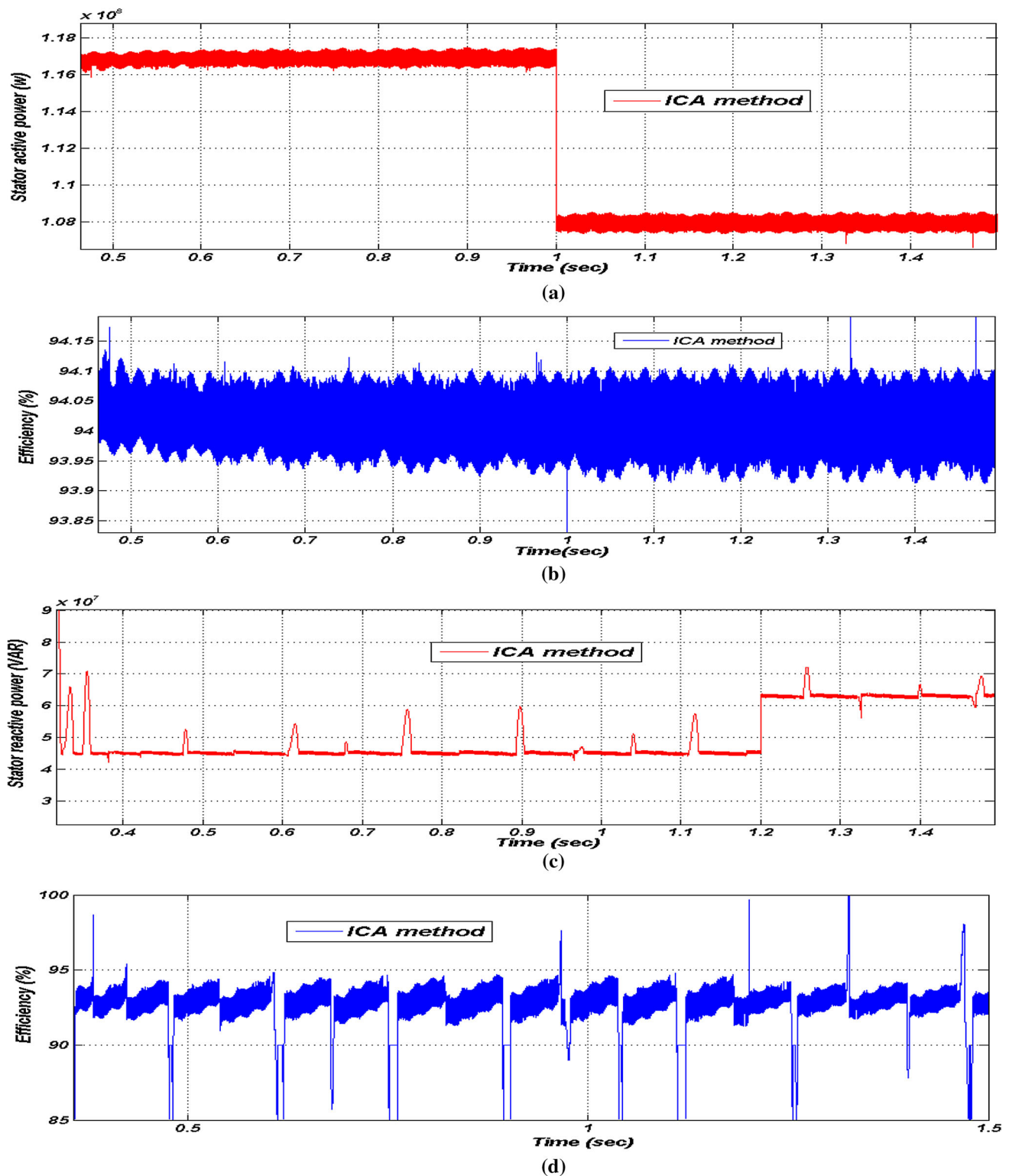


**Fig. 14** a Variations in the stator active power in the method based on ICA; b efficiency of the stator active power in the method based on ICA; c variations in the stator's reactive power in the method based on ICA; d efficiency of the stator's reactive power in the method based on ICA

on the PSO for the iterations needed to run as well as the initial population size mentioned in Table 6 is about 87,350 s. The run time for the method based on the ICA

with the conditions stated in Table 7 is about 27,300 s. The run time for the method based on the TLBO with the conditions stated in Table 8 is about 22,700 s. It is clear



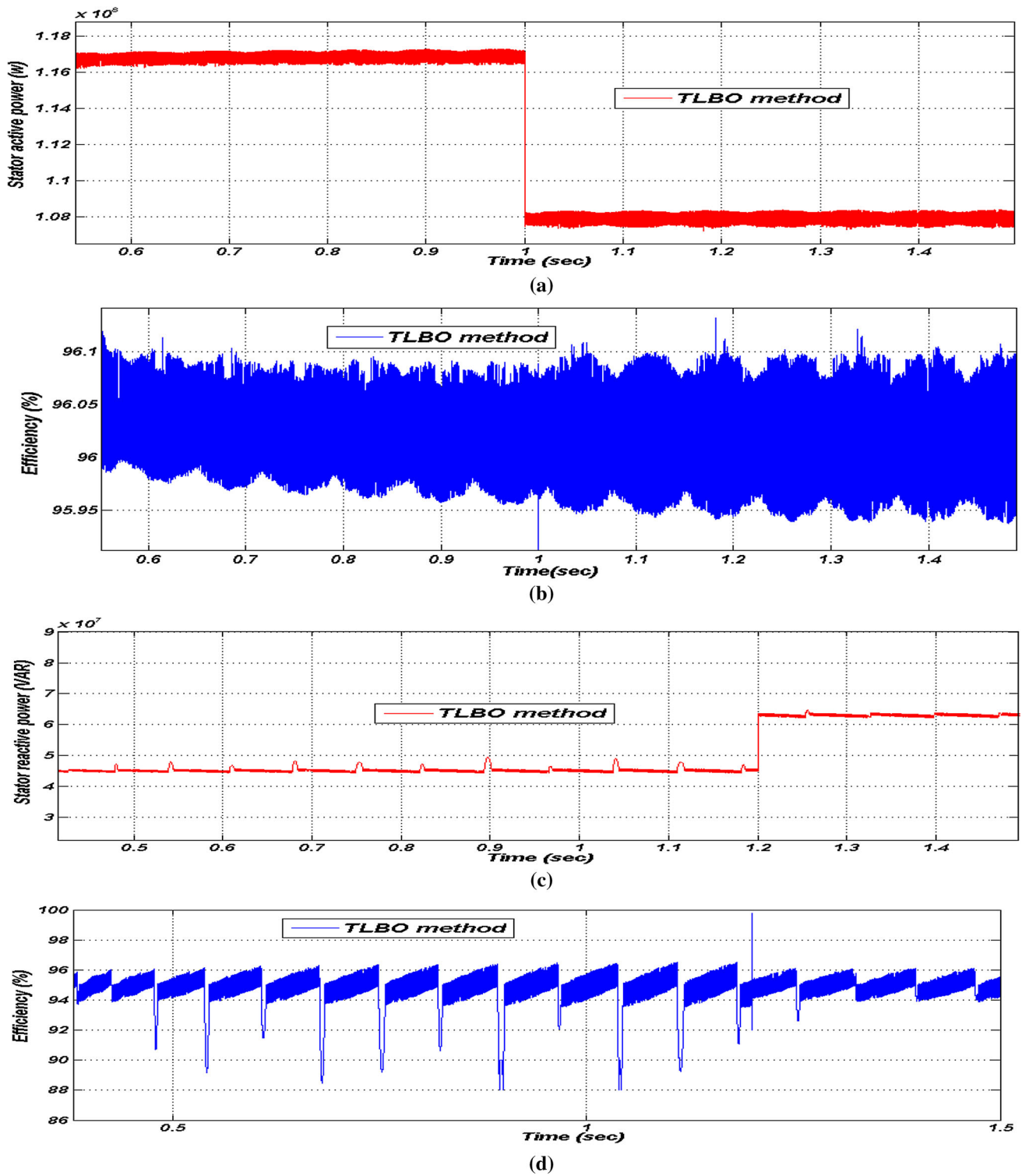
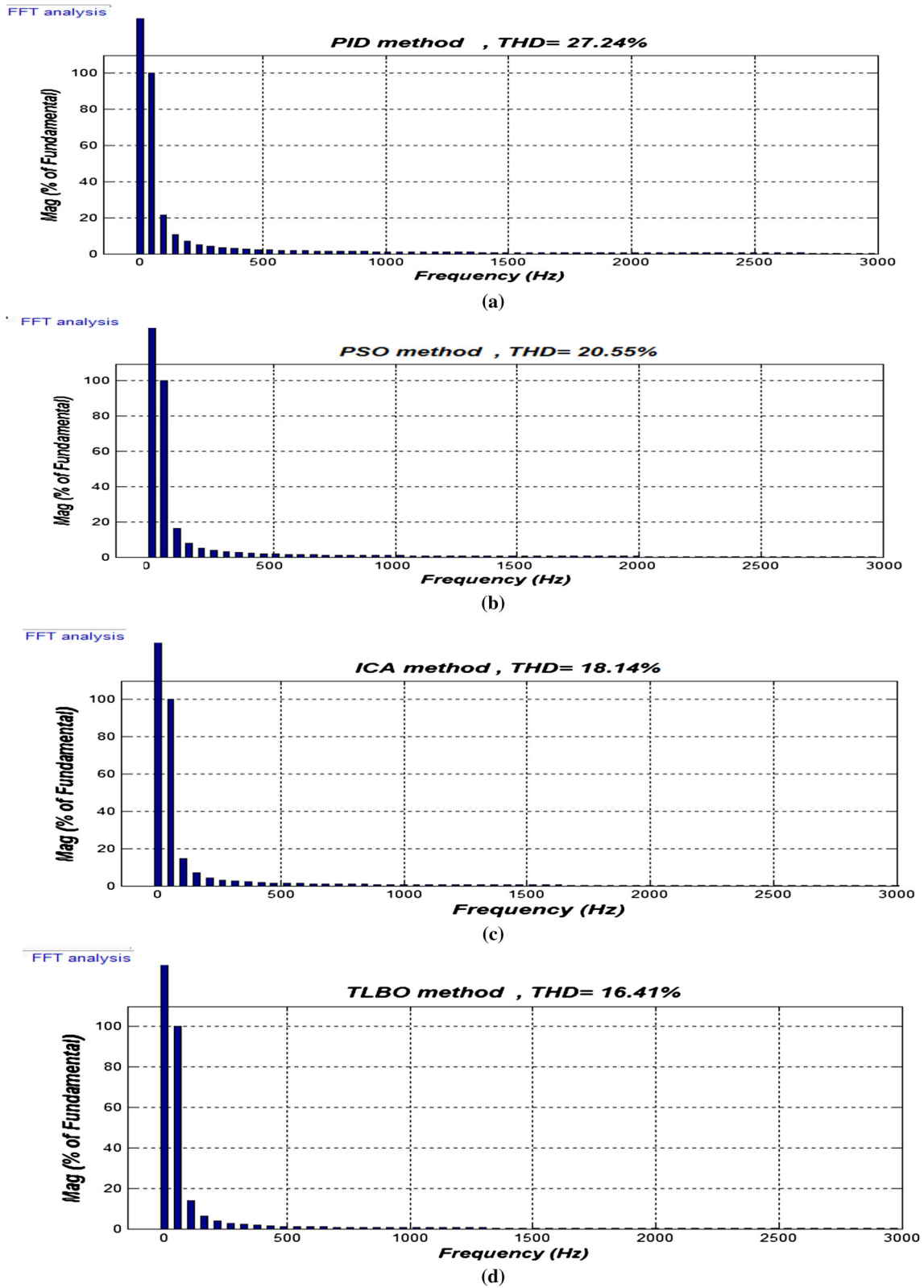


Fig. 15 a Variations in the stator’s active power in the method based on TLBO; b efficiency of the stator’s active power in the method based on TLBO; c variations in the stator’s reactive power in the

method based on TLBO; d efficiency of the stator’s reactive power in the method based on TLBO

that the number of iterations and the initial population stated in this paper cannot lead to the ideal answer. It is expected that when computer systems with a higher

processing capability are used, further iterations and initial population can be assigned to the model resulting in better results. Simulation results show that the proposed approach



**Fig. 16** **a** THD value for rotor current in the method based on PID controller; **b** THD value for rotor current in method based on the PSO; **c** THD value for the rotor current in method based on ICA; **d** THD value for rotor current in the method based on TLBO

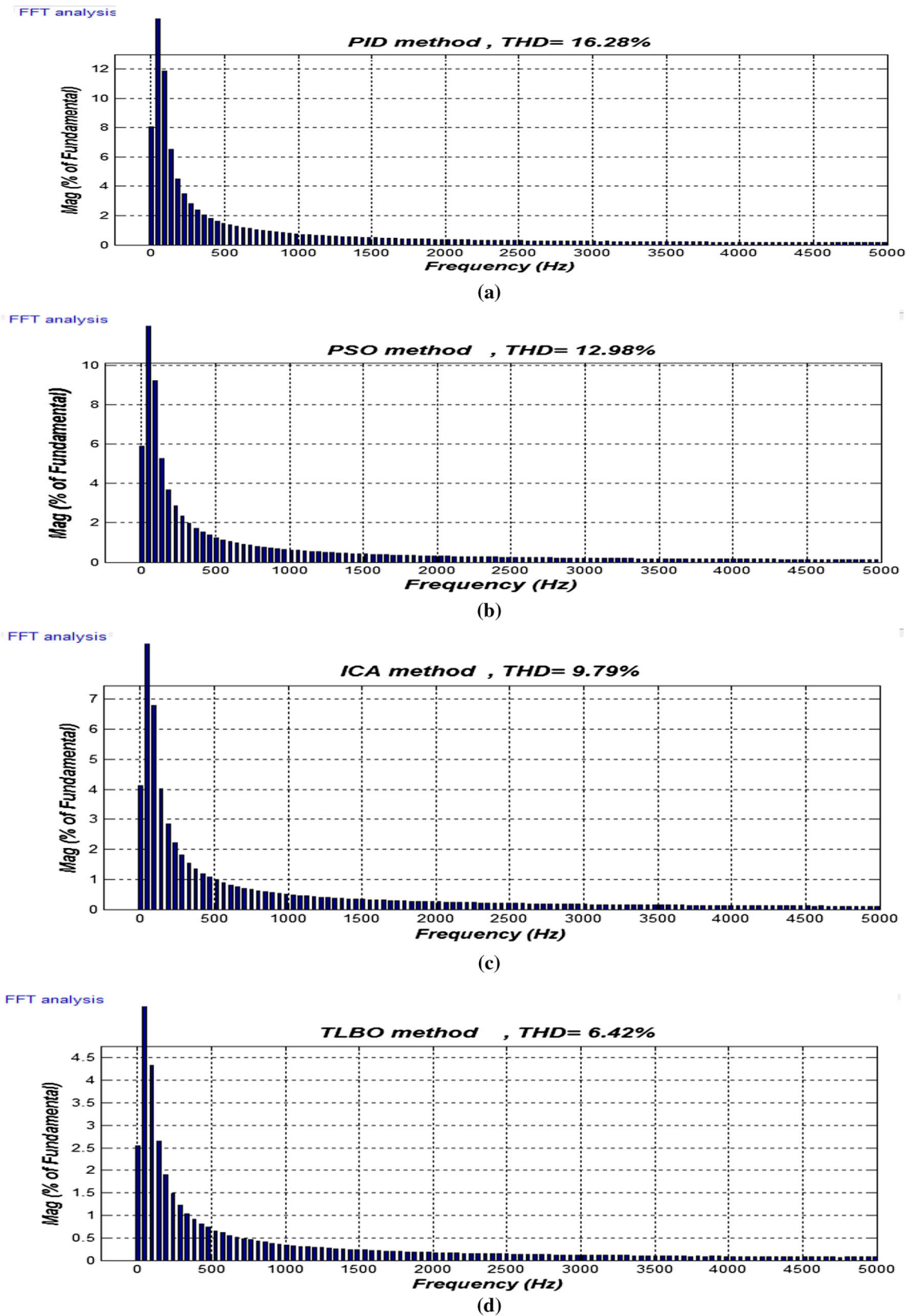


Fig. 17 a THD value for stator current in the method based on the PID controller; b THD value for stator current in the method based on PSO; c THD value for stator current in the method based on ICA; d THD value for stator current in the method based on TLBO

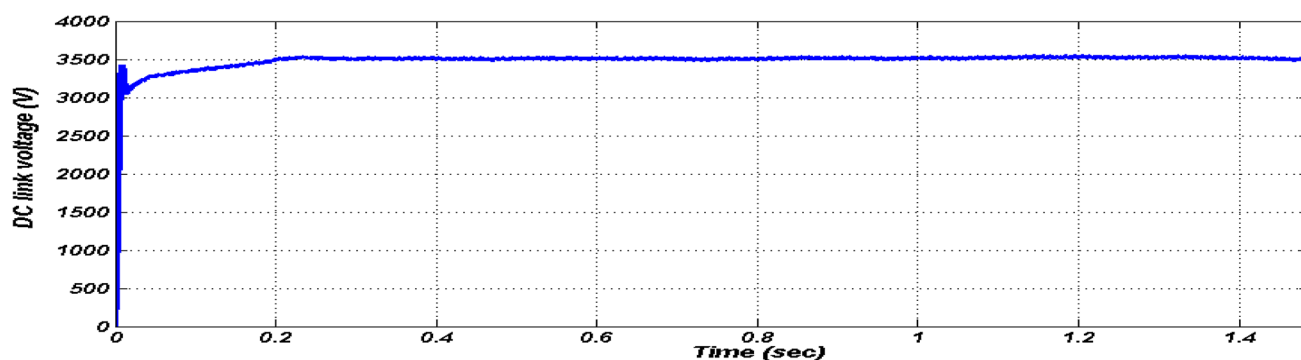


Fig. 18 DC link voltage applied to the inverter

**Table 10** Comparison of system dynamic behavior

Method Parameter	PID	PSO	ICA	TLBO
Stator current THD	16.28%	12.98%	9.79%	6.42%
Rotor current THD	27.24%	20.55%	18.14%	16.41%
Average efficiency of active power	90.2%	92.3%	94.07%	96.02%
Average efficiency of reactive power	87.3%	91.4%	93.7%	95.6%
RMS stator voltage (PU)	0.9826	0.9844	0.9815	0.9906
RMS rotor voltage (PU)	0.1726	0.1814	0.1855	0.1865
RMS stator current (PU)	0.6223	0.6525	0.7239	0.7345
RMS rotor current (PU)	0.1314	0.1455	0.1634	0.1747

is efficient in finding the optimal parameters of the PID controllers, and therefore, it improves the transient performance of the PS plant over a wide range of operating conditions.

## 11 Conclusion

In this paper, a doubly fed induction machine together with a back-to-back converter in a PS plant was modeled and the direct power control (DPC) technique was used to control the machine to eliminate the power ripple and current harmonic. The space vector machine (SVM) method was also utilized in the switching. Considering that the control coefficients  $K_I$  and  $K_P$  in the PI controller employed in the SVM method need to be tuned, three intelligent approaches, namely particle swarm optimization (PSO), imperialist competitive algorithm (ICA) and teaching–learning-based optimization (TLBO), have been used to this end and a comparison was made between the results obtained from the three approaches. The comparison showed that using TLBO algorithm to adjust coefficients would improve the power quality by reducing the active as well as the reactive power ripple of the stator. Moreover, in the case of utilizing the tuned coefficients obtained by TLBO method, the total

harmonic distortion (THD) of the rotor and stator currents is less than the case with PSO and ICA. However, it should be noted that the results are derived using a very small number of iterations and initial population that was due to the long run time.

## Compliance with ethical standards

**Conflict of interest** The authors declare that they have no competing of interest.

## References

- Abad G, Rodriguez MA, Poza J (2007) Predictive direct power control of the doubly fed induction machine with reduced power ripple at low constant switching frequency. In: IEEE international symposium on industrial electronics, ISIE, pp 1119–1124
- Abido MA (2002) Optimal design of power-system stabilizer using particle swarm optimization. IEEE Trans Energy Convers 17(3):406–413
- Atashpaz E, Lucas C (2007) Imperialistic competitive algorithm for optimization inspired by imperialistic competition. In: 2007 IEEE congress on evolutionary computation (CEC 2007), pp 4664–4667

- Cai WW, Jia LX, Zhang YB (2010) Design and simulation of intelligent PID controller based on particle swarm optimization. In: E-Produce E-Service E-Entertainment (ICEEE), Henan
- Chatterjee SH, Mukherjee V (2016) PID controller for automatic voltage regulator using teaching–learning based optimization technique. *Electr Power Energy Syst* 77:418–429
- Dadfar S, Wakil K, Khaksar M, Rezvani A, Miveh MR, Gandomkar M (2019) Enhanced control strategies for a hybrid battery/photovoltaic system using FGS-PID in grid-connected mode. *Int J Hydrogen Energy* 44(29):14642–14660
- Dendouga A, Abdessemed R, Bendas M, Chaiba A (2007) Decoupled active and reactive power control of a doubly fed induction generator (DFIG). In: Mediterranean conference on control and automation, Athens
- Farajdadian S, Hosseini SMH (2019) Design of an optimal fuzzy controller to obtain maximum power in solar power generation system. *Sol Energy* 182:161–178
- Hasanien HM, Muyeen SM (2012) Design optimization of controller parameters used in variable speed wind energy conversion system by genetic algorithms. *IEEE Trans Sustain Energy* 3(2):200–208
- Hosseini SMH, Eslami S (2019) Modelling of PSPP control system by using vector control principle and VSI. In: 5th International conference on power generation systems and renewable energy technologies (PGSRET), 26–27 Aug 2019, Turkey
- Hosseini SMH, Semsar MR (2016) A novel technology for control of variable speed pumped storage power plant. *J Central South Univ* 23(8):2008–2023
- Ju P, Handschin E, Reyer F (1996) Genetic algorithm aided controller design with application to SVC. *IEE Proc Gener Transm Distrib* 143(3):258–262
- Kennedy J, Eberhart R (1995) Particle swarm optimization. In: Proc. IEEE. int. conf. neural networks, vol 4, pp 1942–1948
- Lansberry JE, Wozniak L (1994) Adaptive hydrogenator governor tuning with a genetic algorithm. *IEEE Trans Power Syst* 9(1):179–183
- Muller S, Deicke M, De Doncker RW (2002) Doubly fed induction generator system for wind turbines. *IEEE Ind Appl Mag* 8(3):26–33
- Ou C, Lin W (2006) Comparison between PSO and GA for parameters optimization of PID controller. In: Proceeding of the 2006 IEEE international conference on mechatronics and automation
- Pannatier Y, Kawkabani B, Nicolet C, Simond J, Schwery A, Allenbach P (2010) Investigation of control strategies for variable-speed pump-turbine units by using a simplified model of the converters. *IEEE Trans Ind Electron* 57:3039–3049
- Pena R, Clare JC, Asher GM (1996) Doubly fed induction generator using back-to-back PWM converters and its application to variable speed wind-energy generation. *IEE Proc Electr Power Appl* 143(3):231–241
- Qiao W, Venayagamoorthy GK, Harley RG (2006) Design of optimal PI controllers for doubly fed induction generators driven by wind turbines using particle swarm optimization. In: 2006 Int. joint conf. on neural networks, Vancouver, BC, pp 1982–1987
- Rai D (2017) Comments on “A note on multi-objective improved teaching-learning based optimization algorithm (MO-ITLBO)”. *Int J Ind Eng Comput* 8(2):179–190
- Rao RV, Savsani VJ, Vakharia DP (2011) Teaching–learning-based optimization: a novel method for constrained mechanical design optimization problems. *Comput Aided Des* 43(1):303–315
- Rezvani A, Khalili A, Mazareie A, Gandomkar M (2016) Modeling, control, and simulation of grid connected intelligent hybrid battery/photovoltaic system using new hybrid fuzzy-neural method. *ISA Trans* 1(63):448–460
- Rezvani A, Esmaeily A, Etaati H, Mohammadinodoushan M (2019) Intelligent hybrid power generation system using new hybrid fuzzy-neural for photovoltaic system and RBFNSM for wind turbine in the grid connected mode. *Front Energy* 13(1):131–148
- Schmidt J, Kemmettmuller W, Kugi A (2017) Modeling and static optimization of a variable speed pumped storage power plant. *Renew Energy*. <https://doi.org/10.1016/j.renene.2017.03.055>
- Tang T, Xu L (1995) A flexible active reactive power control strategy for a variable speed constant frequency generating system. *IEEE Trans Power Electron* 10(4):472–477
- Tapia A, Tapia G, Ostolaza JX, Saenz JR (2003) Modeling and control of a wind turbine driven doubly fed induction generator. *IEEE Trans Energy Convers* 18(2):194–204
- Wu F, Zhang XP, Godfrey K, Ju P (2007) Small signal stability analysis and optimal control of a wind turbine with doubly fed induction generator. *IET Gener Transm Distrib* 1(5):751–760
- Yamamoto M, Motoyoshi O (1991) Active and reactive power control for doubly-fed wound rotor induction generator. *IEEE Trans Power Electron* 6(4):624–629

**Publisher's Note** Springer Nature remains neutral with regard to jurisdictional claims in published maps and institutional affiliations.